J Appl Physiol 108: 128–136, 2010.
First published November 5, 2009; doi:10.1152/japplphysiol.00729.2009.

Multivariate adaptive regression splines models for the prediction of energy expenditure in children and adolescents

Issa F. Zakeri,[1] Anne L. Adolph,[2] Maurice R. Puyau,[2] Firoz A. Vohra,[2] and Nancy F. Butte[2]

[1]*Department of Epidemiology and Biostatistics, Drexel University, Philadelphia, Pennsylvania; and* [2]*US Department of Agriculture/Agricultural Research Service, Children's Nutrition Research Center, Department of Pediatrics, Baylor College of Medicine, Houston, Texas*

Submitted 7 July 2009; accepted in final form 5 November 2009

Zakeri IF, Adolph AL, Puyau MR, Vohra FA, Butte NF. Multivariate adaptive regression splines models for the prediction of energy expenditure in children and adolescents. *J Appl Physiol* 108: 128–136, 2010. First published November 5, 2009; doi:10.1152/japplphysiol.00729.2009.—Advanced mathematical models have the potential to capture the complex metabolic and physiological processes that result in heat production or energy expenditure (EE). Multivariate adaptive regression splines (MARS) is a nonparametric method that estimates complex nonlinear relationships by a series of spline functions of the independent predictors. The specific aim of this study is to construct MARS models based on heart rate (HR) and accelerometer counts (AC) to accurately predict EE, and hence 24-h total EE (TEE), in children and adolescents. Secondarily, MARS models will be developed to predict awake EE, sleep EE, and activity EE also from HR and AC. MARS models were developed in 109 and validated in 61 normal-weight and overweight children (ages 5–18 yr) against the criterion method of 24-h room respiration calorimetry. Actiheart monitor was used to measure HR and AC. MARS models were based on linear combinations of 23–28 basis functions that use subject characteristics (age, sex, weight, height, minimal HR, and sitting HR), HR and AC, 1- and 2-min lag and lead values of HR and AC, and appropriate interaction terms. For the 24-h, awake, sleep, and activity EE models, mean percent errors were -2.5 ± 7.5, -2.6 ± 7.8, -0.3 ± 8.9, and $-11.9 \pm 17.9\%$, and root mean square error values were 168, 138, 40, and 122 kcal, respectively, in the validation cohort. Bland-Altman plots indicated that the predicted values were in good agreement with the observed TEE, and that there was no bias with increasing TEE. Prediction errors for 24-h TEE were not statistically associated with age, sex, weight, height, or body mass index. MARS models developed for the prediction of EE from HR monitoring and accelerometry were demonstrated to be valid in an independent cohort of children and adolescents, but require further validation in independent, free-living populations.

accelerometers; heart rate monitoring; calorimetry; total energy expenditure; sleep energy expenditure; physical activity

ENERGY EXPENDITURE (EE) REPRESENTS energetic processes required to support the metabolic activities of cells and tissues, vital organ functions, and volitional and spontaneous physical activity. Although accurate, direct and indirect calorimetric methods that measure heat or respiratory exchange can be intrusive, confining, and expensive, and thus impractical for large-scale studies. Consequently, alternative approaches based on physiological correlates of EE have been developed (3, 5, 24). These ambulatory methods use small, relatively inexpensive wearable devices, such as accelerometers and heart rate (HR) monitors, and have been successful in the prediction of EE for groups, but less so for individuals. Multiple sensors and advanced mathematical modeling techniques have the potential to capture the complex metabolic and physiological processes that result in heat production or EE and to improve on the prediction of EE.

The combination of accelerometers and HR monitors has been shown to improve the accuracy and precision of EE predictions (2, 14, 19–21, 26). However, the mathematical modeling of the HR and accelerometer counts (AC) to predict EE was limited to simple linear regression or branched equation modeling that do not take into account the complex, dynamic, and nonlinear relationships between EE, HR, and AC over time. Nonlinear methods, such as artificial neural network (ANN), have been used both for classification of activity mode and prediction of EE (16, 26, 27). A probabilistic ANN was used to extract information about the type, duration, and intensity of activity from the IDEEA multiple sensor system, which, together with energy cost of activities, was used to predict EE (26, 27). Raw signals from a biaxial accelerometer and subject characteristics were used to develop an ANN model for the prediction of minute-by-minute EE in 102 young adults (16). Recently, we applied a parametric model, cross-sectional time series (CSTS) analysis, for the prediction of EE from HR and AC (25). This approach is transparent and accounts for the interdependence of EE, HR, and AC over time.

Here within, we apply another modern statistical technique to predict EE called multivariate adaptive regression splines (MARS) (8). MARS is a nonparametric regression method that approximates a complex nonlinear relationship by a series of spline functions on different intervals of the independent variable. A key property of MARS over global parametric models, such as CSTS, is its ability to operate locally. MARS allows inclusion of interaction terms, which are active in a localized region of the variables involved. In other words, different subregions of predictors might have different interaction patterns. MARS can be viewed as a generalization of binary recursive partitioning, which includes branched equation modeling, since it overcomes some of the limitations of recursive partitioning. For example, in recursive partitioning, the subregions are disjointed, and, as a result, the approximating functions are discontinuous at the subregion boundaries, which severely limits the accuracy of the approximation in particular when the underlying function is continuous. However, MARS has overlapping subregions, and it produces a continuous model for continuous predictors. MARS results in a class of models

Address for reprint requests and other correspondence: N. F. Butte, Children's Nutrition Research Center, Baylor College of Medicine, 1100 Bates St., Houston, TX 77030 (e-mail: nbutte@bcm.edu).

with greater flexibility than permitted in recursive partitioning. MARS is computationally feasible due to recent advances in statistical computing and may provide an effective tool to obtain better predictive models for EE.

The primary objective of this study is to develop and validate MARS models based on HR, AC monitoring, and individual characteristics to accurately predict minute-by-minute EE, and hence 24-h total EE (TEE) in children and adolescents against the criterion method of room respiration calorimetry. Secondarily, MARS modeling will be applied to predict awake EE, sleep EE, and activity EE from HR and AC.

MATERIALS AND METHODS

Study design. A two-stage study design, including a development phase and a validation phase, was employed. HR and AC were measured simultaneously with measurements of minute-by-minute EE while inside a room respiration calorimeter for 24 h, in 109 children and adolescents for the development phase, and in 61 children and adolescents for the validation phase. The inclusion criteria required the children to be healthy and free from any medical condition that would limit participation in physical activity. The Institutional Review Board for Human Subject Research for Baylor College of Medicine and Affiliated Hospitals approved the protocol. All parents gave written, informed consent to participate in this study.

Subjects. The characteristics of the children who took part in the study are presented in Table 1. Subjects represented white, black, Hispanic, and Asian children and the age range of 5–18 yr. Forty-eight children in the development group and twenty-six children in the validation group were classified as overweight by the Centers for Disease Control growth charts (11).

Anthropometry. Body weight to the nearest 0.1 kg was measured with a digital balance, and height to the nearest 1 mm was measured with a stadiometer. Body mass index (BMI) was calculated as weight/height^2 (kg/m^2).

Physical activity-HR monitor. The Actiheart (MiniMitter, Respironics, Bend, OR) monitor was secured to the chest of each subject with two electrodes. Actiheart is a compact (7-mm thick, 33-mm diameter, 10-g total weight), ambulatory device equipped with an omnidirectional accelerometer and ECG signal processor. The accelerometer contains a piezoelectric transducer, whose motion sensitivity is greatest along the preferred axis (vertical, when worn as prescribed) but which will produce lesser signals when the motion is perpendicular to the preferred axis. The memory capacity of 128 kb allows data storage for 11 days for the 15-s epoch setting. The piezoelectric element (frequency range 1–7 Hz) generates a transient charge when exposed to time-varying acceleration. This produces a voltage signal, which is converted into a binary signal, resulting in 256 distinct levels of acceleration. The dynamic range of the accelerometer is ± 25 m/s^2 (± 2.5 G), and its sensitivity per bit is approximately one count per 0.025 G, or one count per 0.23 m/s^2. The binary signal is summed up over a 15-s epoch. Actiheart digitizes the ECG signal and calculates the HR from the interbeat interval (IBI). It detects the QRS complex by identifying the location of the R-wave line of steepest descent. The logger firmware applies a digital threshold for this differential value that compensates for variation in the signal level due to physiological changes, noise, and physical movement. Sixteen consecutive IBIs are measured, and the average of the 16 intervals is calculated. Any of the IBI values that are >37.5% of the average are identified and discarded. The average IBI is recalculated, and its inverse is multiplied by 60 to obtain the HR. Note: The activity counts output of the MiniMitter Actiheart and CamNtech Actiheart (CamNtech, Cambridge, UK) differ slightly. To utilize the MARS equations in this paper, the activity counts from the CamNtech unit should be multiplied by 5/6 to achieve the same value as the MiniMitter unit (per CamNtech).

Before each test, the calibration of the Actiheart device is confirmed using the Motion Performance Verification System (MiniMitter, Philips Respironics, Bend, OR). Variability of PA measurements both within and between Actiheart monitors was tested using repeated measurements on the Motion Performance Verification System. Intramonitor coefficient of variation was found to be 1.3% and intermonitor coefficient of variation was 4.3% for the eight Actiheart units used in this study. HR measurements of the Actiheart monitors were in perfect agreement with an ECG simulator (Dale Technology, Thornwood, NY) operating at rates of 60 and 120 beats/min. The mean agreement between HR independently measured by the Fukuda instrument and Actiheart was 0.2 ± 0.1% for all subjects.

The Actiheart was affixed on the chest using electrodes (Skintact Premier, Leonhard Lang, Innsbruck, Austria). The main sensor was attached left of the sternum and secured with the adhesive tab on the electrode. The lead was attached parallel along the midclavicular line at the level of the third intercostal space (upper position) or just below the left breast (lower position). Throughout the study, the electrodes were checked and replaced if there was poor adhesion.

At the conclusion of the study, the data were downloaded into Excel. HR and PA data acquisition by Actiheart is set at 15-s intervals. Actiheart data were collapsed into 60-s intervals and aligned with the minute-by-minute EE data. HR data were filtered with an upper cutoff of 240 beats/min and a lower cutoff set at 10 beats/min below the subject's average sleeping HR. For invalid or missing HR values in the development (4.2%) and validation (1.5%) cohorts, HR values measured in the calorimeter by telemetry (DS-3000, Fukuda Denshi) were substituted. In both cohorts, 75% of the subjects had <10 min of invalid or missing HR. Minute-by-minute EE were summed for discrete physical activities and 24-h periods. Awake and sleep HR were calculated as the average HR for the entire times during which the subject was awake and sleeping. Minimal HR (MinHR) was determined to be the lowest 20-min average of HR during sleep. Sitting HR (SitHR) was the average HR for a 10-min period while the subject was sitting in the upright position watching television.

Room respiration calorimetry. During the 24-h calorimetry, continuous measurements of EE and activity were collected while the children completed a series of physical activities, and also while sleeping and eating. Oxygen consumption and carbon dioxide pro-

Table 1. *Subject description*

	Boys	Girls	All
	Development cohort		
n	61	48	109
Age, yr	12.0 ± 3.3	12.7 ± 3.8	12.3 ± 3.5
Race/ethnicity (w/b/h/a), %	23/25/47/5	33/23/44/0	28/24/46/2
Weight, kg	55.7 ± 24.9	58.2 ± 25.7	56.8 ± 25.2
Height, m	1.51 ± 0.19	1.50 ± 0.16	1.51 ± 0.18
BMI *z*-score	0.97 ± 1.28	1.10 ± 1.20	1.03 ± 1.24
Overweight (BMI ≥95th percentile), %	41	46	44
	Validation cohort		
n	35	26	61
Age, yr	11.7 ± 4.0	11.8 ± 3.7	11.8 ± 3.8
Race/ethnicity (w/b/h/a), %	20/31/49/0	19/23/54/4	20/28/51/1
Weight, kg	57.8 ± 28.8	52.5 ± 17.9	55.6 ± 24.7
Height, m	1.52 ± 0.24	1.48 ± 0.17	1.50 ± 0.21
BMI *z*-score	1.00 ± 1.22	1.17 ± 1.14	1.08 ± 1.18
Overweight (BMI ≥95th percentile), %	34	54	43

Values are means ± SD; *n*, no. of subjects. w, white; b, black; h, Hispanic; a, Asian; BMI, body mass index.

duction were measured continuously in a 30-m^3 room calorimeter. The performance of the respiration calorimeters has been described previously (15). EE was computed using the Weir equation (23). Oxygen consumption, carbon dioxide production, EE, and HR were averaged at 1-min intervals.

A series of physical activities was completed under supervision in the same order between 9:00 AM and 5:00 PM, with "free-time" and meal time in between measurements. Specific measurements obtained in the room calorimeter included the following: working on a computer for 20 min while sitting in a chair; playing PlayStation 2 games for 20 min in a sitting position; playing Eye Toy in the standing position for 15 min; performing aerobic exercises, as demonstrated on a videotape for 20 min; watching a movie while sitting in a lounge chair for 90 min; sitting in the lounge chair while watching television for 20 min; sitting and assembling a floor puzzle for 15 min; dancing to music for 15 min; basal metabolic rate (BMR) measured under thermoneutral conditions (22–24°C) upon awakening after a 12-h fast for 30 min; and four 10-min sessions on the treadmill (model C942, Precor, Woodinville, WA) set according to the age, capability, and safety of the children, including a slow walk, a 2.5-mph walk, and a fast walk/jog. Activity EE during the awake period was defined as EE-BMR-0.1 EE, assuming that the thermic effect of food is equal to 10% of EE. Except for the BMR measurement, all activities were performed in the fed state. The children were given breakfast at 8:30 am, lunch at 12:00 pm, a snack at 2:45 pm, and dinner at 5:30 pm.

In the validation protocol, unlike the development protocol, some choices were given to the children in completing supervised activities. As in the development protocol, children completed a BMR measurement and watched a movie. Instead of Eye Toy and dancing, each child played the Wii Sports (bowling, tennis, and boxing) and Dance Dance Revolution video games at their own skill level for 20–30 min each. Two 20-min treadmill sessions were performed where the child selected his or her own speed for a slow walk and a fast walk/jog. In addition, all children walked for 20 min at 2.5 mph.

MARS modeling. The MARS procedure is a nonparametric, spline-based method and makes no assumptions about the underlying functional relationship between the dependent and independent variables. Splines have characteristics that make them important tools for approximating functions or data fitting and numerical analysis. Polynomial splines are at the heart of many techniques for nonparametric regression and function estimation and provide an effective approach to modern nonparametric modeling (7, 22).

The basic idea behind spline models is to allow potentially different functions (linear or nonlinear) over different intervals. The end points of the intervals are called knots, a key concept underlying spline models. A knot marks the end of one region of data and the beginning of another. The resulting piecewise curve is called a spline. Typically, the end points of the intervals or the locations where the lines or curves meet or are tied together are unknown and must be estimated. MARS is an adaptive procedure for regression and provides an algorithm for selecting possible knot locations.

To explain this type of modeling, let (y_{ij}, x_{ij}), $i = 1, \ldots, N$, $j = 1, \ldots, n_i$, be the measured minute-by-minute EE and predictors at the jth time point for the ith individual, respectively, where $x_{ij} = (x_{ij1}, \ldots, x_{ijp})$ denotes the vector of p possible predictors or covariates, including HR and AC. The aim is to model the dependence of y_{ij} on x_{ij}, which is capable of representing the complex nonlinear relationship. The basic model that we shall consider is that the minute-by-minute EE, y_{ij}, of the ith child are generated by an unknown "smooth" function f and additive noise ε_{ij}. More specifically, we will investigate the following nonparametric regression model:

$$y_{ij} = f(x_{ij}) + \varepsilon_{ij} \quad (1)$$

where the error terms ε_{ij} are mean zero random variables. The aim here is to estimate the unknown function f, assuming as little as possible about its specific form, based on the available data, such that the resultant function is a good approximation and can perform well over the domain of interest.

For notational convenience, we write models here as if there were one series of observations [the data are (y_i, x_i), $x_i = (x_{i1}, \ldots, x_{ip})$, $i = 1, \ldots, N$]. Splines are generally defined to be piecewise polynomial functions of some degree $q > 0$, the highest power defining the polynomial. The breakpoints marking the transition from one polynomial to the next are referred to as knots (or joint points). For example, a polynomial spline function of degree $q > 0$ for a predictor say x with k knots at $t_1, \ldots, t_k$ can be represented using the following basis functions:

$$1, x, \ldots x^q, (x - t_1)_+^q, \ldots, (x - t_k)_+^q \quad (2)$$

where the "+" means the positive part, so $(x - t)_+$ is equal to $(x - t)$ if $x > t$ and is equal to zero otherwise. The set in *Eq. 2* is called the truncated power basis of degree q. The set can also be generated using the leftsided truncated basis function $(t - x)_+^q$. Since the function $(x - t)_+^q$ has $q - 1$ continuous derivatives, higher values of q lead to smoother functions.

Truncated power bases are very useful for understanding the mechanism of spline-based regression. In general, it is possible to handle any complex type of data structure by simply adding more truncated functions to the basis, that is, by increasing the number of knots. However, that might lead to overfitting the data, meaning that the fitted function is following random fluctuations in the data as well as the main features. One could, of course, try pruning the knots to overcome this problem.

Spline-based models require consideration of the degree of polynomials, the number of knots, and the location of knots. The MARS method uses linear truncated power functions as spline basis functions, i.e., fitting of splines of *order 1* to each variable. Therefore, the collection of the basis functions is $C = \{(x_j - t)_+, (t - x_j)_+\}$ for $j = 1, \ldots, p$ and t is an observed value of the predictor x_j. In principal, a change of basis does not change the fit, but some bases are more numerically stable and allow computation of fit with greater accuracy. Linear truncated splines are simple and allow rapid updating of the regression model and its coefficients as the knot position is changed.

The fundamental idea of MARS is to use the combination of the linear truncated basis functions to approximate the model. Thus the functions of MARS consist of single spline functions or the product of two or more of the truncated power functions to allow for the interactions. This allows both the additive and the interactive effects of the predictors in determining the response variable. The MARS estimate of the unknown regression function $f(x)$ can be written as an additive function of the product basis functions:

$$f_M(x) = \beta_0 + \sum_{m=1}^{M} \beta_m B_m(x) \quad (3)$$

where β_0 is the coefficient of the constant basis function $B_0(x) = 1$, $B_m(x)$ is the mth basis function, which may be a single spline function or product of two or more, β_m is the coefficient of the basis function, and M is the number of basis functions in the model. For a given set of basis functions, the unknown parameters in MARS can be determined easily using the least squares criterion (9).

The MARS algorithm starts with the constant basis function $B_0(x)$ in the model. Then, successively at each state, a pair of basis functions are added to the model that produces the largest decrease in residual sum of squares by considering all possible pairs of new basis functions: $B_m(x)(x_j - t)_+$ and $B_m(t - x_j)_+$, where x_j is one of the predictors and t is a new knot in that predictor, and $B_m(x)$ is a basis function currently in the model that does not depend on x_j. For example, let x_1 and x_2 denote two predictors, for example HR and AC, and let t_1 and t_2 be two knots from their observed values, respectively. The product functions, such as $(x_1 - t_1)_+ \cdot (x_2 - t_2)_+$, will be included in the model to determine whether the effect of a predictor on EE may depend on the value of another predictor, or whether their joint effect on EE

Table 2. *Observed EE, heart rate, and physical activity of the children and adolescents during the 24-h in the room respiration calorimeter*

	Development	Validation
n	109	61
24-h TEE		
kcal	2,168 ± 591	2,125 ± 664
kcal/min	1.60 ± 0.41	1.54 ± 0.45
Awake EE		
kcal	1,709 ± 511	1,670 ± 557
kcal/min	1.97 ± 0.50	1.85 ± 0.54
Activity EE		
kcal	691 ± 243	611 ± 242
kcal/min	0.79 ± 0.25	0.68 ± 0.24
Sleep EE		
kcal	459 ± 116	456 ± 128
kcal/min	0.94 ± 0.23	0.94 ± 0.26
24-h Heart rate, beats/min	88 ± 9	85 ± 11
Awake heart rate, beats/min	97 ± 10	94 ± 12
Sleep heart rate, beats/min	72 ± 9	70 ± 11
Minimal heart rate, beats/min	64 ± 9	62 ± 10
Sitting heart rate, beats/min	86 ± 10	85 ± 11
24-h Accelerometer counts, counts/min	79 ± 35	39 ± 14
Awake accelerometer counts, counts/min	123 ± 54	60 ± 21
Sleep accelerometer counts, counts/min	1 ± 2	1 ± 1

Values are means ± SD; *n*, no. of subjects. EE, energy expenditure; TEE, total EE.

depends on both predictors being above certain thresholds. This can aid in building a predictive model for EE, since the linear splines operate locally, and the product term is nonzero only over the small part of the input space where both components are nonzero.

The MARS algorithm searches for all possible knot locations for each variable. The forward stepwise addition procedure can produce a large collection of basis functions, and the process is stopped when a user-specified maximum model size is reached. Then a backward pruning procedure is applied to remove one at a time any nonconstant basis functions that no longer make sufficient contribution to the model. The best-fitting model in stepwise sequence is chosen to minimize the generalized cross-validation criterion of Craven and Wahba (6):

$$GCV(M) = \frac{\sum_{i=1}^{N} [y_i - f_M(x_i)]^2}{N[1 - (C(M)/N)]^2} \quad (4)$$

where N is the number of observations, and $C(M)$ is the cost-complexity measure of a model containing M basis functions. The numerator is the sum of squared residuals from the fitted model, and the denominator contains a penalty for model complexity, which is related to the number of parameters estimated in the model. An empirical rule proposed by Friedman (8) will be used to determine $C(M)$.

MARS was developed using R and Salford Systems. Once we obtain the functional form of the MARS model using Salford System, the basis functions as predictors in linear regression equations were implemented using EXCEL.

MARS model evaluation. Goodness-of-fit methods were used to assess and compare competing models based on their agreement between the observed values and model estimates derived from MARS. We analyzed concordance between the observed and predicted TEE. Concordance between two methods indicates the extent to which measurements made by one of the methods can serve as a surrogate for the other. Bland and Altman recommend a graphical method to assess concordance or agreement between two variables (1). Bland and Altman propose to plot the difference vs. the "true" value or mean of the two methods and the "limits of agreement", which are two horizontal lines indicating mean ± twice standard deviation of intraindividual differences. In our application, the observed TEE measured by calorimetry was taken as the "true" value and used on the *x*-axis.

While the Bland-Altman (1) diagnostic plot of the difference vs. the mean can provide insight into the measurement differences between two methods, it does not provide a single measure of agreement. Krippendorff (10) and Lin (12, 13) considered the concordance correlation coefficient (CCC) that is appropriate for measuring agreement when the data are measured on a continuous scale. The CCC consists of a precision component, the Pearson correlation coefficient, which measures how closely observations lie on the line fit to the data, and an accuracy component, which measures how closely the fitted line deviates from the 45° line through the origin. Therefore, when the concordance correlation is high, with values ranging from 0 to 1.0, we can be more confident about the similarity of the two methods.

Summary statistics. Data are summarized as means ± SD. Descriptive statistics were performed using STATA (release 8.2, StataCorp LP, College Station, TX) and SPSS (release 11.50, SPSS, Chicago, IL).

RESULTS

Subject characteristics. A description of the 109 and the 61 children and adolescents who participated in the development and validation phases of the study, respectively, is summarized in Table 1. By design, subjects represented sex, ages 5–18 yr, and a wide range of body sizes. There were no statistically significant differences between the two cohorts in terms of age, weight, height, or BMI *z*-score. Forty-four percent of the subjects were classified as overweight.

Observed EE, HR, and AC. Mean rates of EE, HR, and AC during the entire 24-h, awake and sleep periods are summa-

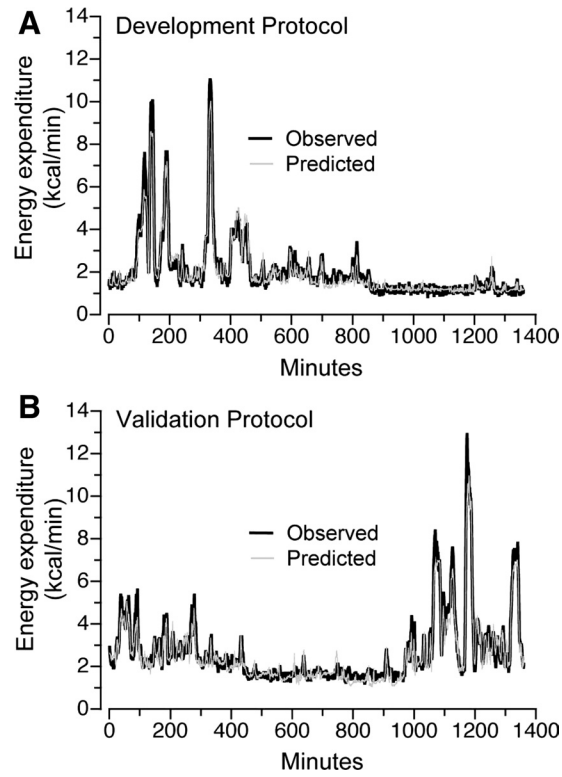

Fig. 1. Predicted vs. observed minute-by-minute energy expenditure (EE) values (kcal/min) for one subject each in the 24-h development (*A*) and validation (*B*) protocols in the room respiration calorimeter.

Table 3. *Basis functions of the 24-h, awake, sleep, and activity MARS models for the prediction of EE*

	24-h EE	Awake EE	Sleep EE	Activity EE
BF1	max (0, AClag1 − 221.48)	max (0, AClag1 − 308.49)	max (0, Weight − 61.2)	max (0, AClag1 − 283.63)
BF2	max (0, 221.48 − AClag1)	max (0, 308.49 − AClag1)	max (0, 61.2 − Weight)	max (0, 283.63 − AClag1)
BF3	max (0, Weight − 61.2)	max (0, Weight − 61.7)	(Gender = 0) * BF1	max (0, Weight − 86.9) * BF1
BF4	max (0, 61.2 − Weight)	max (0, 61.7 − Weight)		max (0, 86.9 − Weight) * BF1
BF5	max (0, AC − 22.6) * BF3	max (0, AC − 36.16) * BF3	max (0, AClag2 − 29.38)	max (0, HRlead2 − 113)
BF6	max (0, 22.6 − AC) * BF3	max (0, 36.16 − AC) * BF3	max (0, 29.38 − AClag2)	max (0, 113 − HRlead2)
BF7	max (0, HRlead2 − 135)	max (0, HRlead2 − 130)	max (0, Age − 17.5)	max (0, Height − 114.7)
BF8	max (0, 135 − HRlead2)	max (0, 130 − HRlead2)	max (0, 17.5 − Age)	max (0, 114.7 − Height)
BF9	max (0, AClag1 − 238.43) * BF4	max (0, AClag1 − 348.04) * BF4	max (0, HR − 76)	max (0, AClag2−125.43) * BF7
BF10	max (0, 238.43 − AClag1) * BF4	max (0, 348.04 − AClag1) * BF4	max (0, 76 − HR)	max (0, 125.43 − AClag2) * BF7
BF11	max (0, AClag2 − 28.25)	max (0, AClag2 − 56.5)	MinHR	max (0, AC − 109.61) * BF7
BF12	max (0, 28.25 − AClag2)	max (0, 56.5 − AClag2)		max (0, 109.61 − AC) * BF7
BF13	MinHR	max (0, Height − 162.2) * BF7	max (0, Height − 160.2)	max (0, Weight − 61.2) * BF7
BF14		max (0, 162.2 − Height) * BF7		max (0, 61.2 − Weight) * BF7
BF15	max (0, Height − 162.2) * BF7	MinHR		max (0, HRlag2 − 132) * BF7
BF16	max (0, 162.2 − Height) * BF7		max (0, 47.460 − AClag1)	max (0, 132 − HRlag2) * BF7
BF17	max (0, AC − 620.37)	max (0, AC − 171.76)	max (0, Weight − 91.3) * BF13	max (0, Height − 162.2) * BF1
BF18	max (0, 620.37 − AC)	max (0, 171.76 − AC)	max (0, 91.3 − Weight) * BF13	max (0, 162.2 − Height) * BF1
BF19	max (0, HRlag2 − 148) * BF3	max (0, HRlag2 − 147) * BF3	max (0, Weight − 81.9) * BF6	max (0, Weight − 49) * BF5
BF20	max (0, 148 − HRlag2) * BF3	max (0, 147 − HRlag2) * BF3	max (0, 81.9 − Weight) * BF6	max (0, 49 − Weight) * BF5
BF21	max (0, Height − 160.2)	(Sex = 0)	max (0, HRlead2 − 73) * BF13	MinHR
BF22	max (0, 160.2 − Height)		max (0, 73 − HRlead2) * BF13	
BF23	(Sex = 0)	max (0, AClag2 − 1,808) * BF21	(Sex = 0) * BF10	
BF24		max (0, 1,808 − AClag2) * BF21		
BF25	max(0, HRlead1 − 112) * BF23	max (0, Height − 157) * BF21	max (0, HRlead1 − 85) * BF6	(Sex = 0) * BF5
BF26	max (0, 112 − HRlead1) * BF23	max (0, 157 − Height) * BF21	max (0, 85 − HRlead1) * BF6	
BF27	max (0, AC − 110.74) * BF21	max (0, SitHR − 83) * BF3		max (0, AC − 724.33) * BF5
BF28	max (0, 110.74 − AC) * BF21	max (0, 83 − SitHR) * BF3		max (0, 724.33 − AC) * BF5
BF29	max (0, SitHR − 78) * BF3	max (0, Weight − 122.5) * BF12	max (0, Age − 13.5) * BF2	max (0, Weight − 30.2) * BF6
BF30	max (0, 78 − SitHR) * BF3	max (0, 122.5 − Weight) * BF12	max (0, 13.5 − Age) * BF2	max (0, 30.2 − Weight) * BF6

Variables used in basis functions (BF) are as follows: Weight (in kg); Height (in cm); Sex (male = 0, female = 1); Age (in yr); HR, minute-by-minute heart rate (in beats/min); MinHR, minimal 20-min average of HR during sleep; SitHR, 10-min average of HR while sitting upright; AC, minute-by-minute accelerometer counts per minute; HRlag2, 2-min lagged value of HR; AClag1 and AClag2, 1- and 2-min lagged values of AC, respectively; HRlead1 and HRlead2, 1- and 2-min lead values of HR, respectively; Max, maximum $(0, x - t) = (x - t)$ when $x > t$ and is otherwise equal to zero. Max $(0, t - x)$ is defined analogously. In our models, functions (BF1–BF30) are used as decision points to determine which value will be used in the multivariate adaptive regression splines (MARS) model at a given knot; for example, for BF1 and BF2, if AClag1 − 221.48 > 0, then BF1 = AClag1 − 221.48; otherwise, if AClag1 − 221.48 < 0, then BF1 = 0. If 221.48 − AClag1 > 0, then BF2 = 221.48 − AClag1; otherwise, if 221.48 − AClag1 < 0, then BF2 = 0.

rized in Table 2 for the development and validation cohorts. The performance of the MARS model is exemplified by the predicted vs. observed minute-by-minute EE values for one subject each in the 24-h development and validation protocols (Figs. 1, *A* and *B*, respectively). Mean physical activity level, defined as the ratio of TEE to BMR, was 1.61 ± 0.15 for the development cohort and 1.54 ± 0.11 for the validation cohort, indicating a slightly higher level of physical activity was achieved in the development cohort, who performed similar tasks at greater intensities. As potential indicators of individual's fitness level, MinHR and SitHR were extracted from individual 24-h files.

Development of MARS models. As a result of our modeling process, the final basis functions utilized subject characteristics, HR and AC, 1- and 2-min lag and lead values of HR and AC, and appropriate interaction terms. Subject-specific variables include age, sex, weight, height, MinHR, and SitHR. First, we examined main effects models and then allowed interaction terms between basis functions. All of the potential knot locations for each of the predictors or main effects were investigated in the developing of the MARS models. For simplicity and ease of interpretation, we only allowed two-way interactions between basis functions, if the model fit substantially improved. Based on the generalized cross-validation criterion (see *Eq. 4*), the "best" model, i.e., optimal number of basis functions and knot locations, was selected.

Prediction models for rates of EE (kcal/min) were developed for the 24-h period (24-h EE), the awake period (awake EE), the sleep period (sleep EE), and activity (activity EE). The final MARS models are based on linear combinations of 28, 28, 26, and 23 basis functions (BF) for 24-h EE, awake EE, activity EE, and sleep EE, respectively. The basis functions are detailed in Table 3.

Table 4. *Prediction errors of the 24-h, awake, sleep, activity and combined MARS models presented as mean absolute error, percent error, and root mean square error in the development cohort*

	Mean Absolute Error, kcal	Percent Error, %	Root Mean Square Error, kcal
24-h Model			
24-h TEE	0.0 ± 155.0	0.4 ± 7.3	154.3
Awake EE	−35.8 ± 130.9	−1.5 ± 7.5	135.1
Sleep EE	35.8 ± 43.5	7.8 ± 10.1	56.2
Awake model			
Awake EE	0.0 ± 122.3	0.4 ± 7.2	121.7
Sleep model			
Sleep EE	0.0 ± 27.1	0.5 ± 6.4	27.0
Activity model			
Activity EE	0.0 ± 108.7	1.5 ± 16.5	108.2
Combined model (awake + sleep) 24-h TEE	−0.1 ± 140.1	0.4 ± 6.7	139.4

Values are means ± SD.

The prediction equations for 24-h EE, awake EE, sleep EE, and activity EE models are as follows:

24-h EE (kcal/min) = 0.0006111*BF1 − 0.0045469*BF2
+0.027344*BF3 − 0.0420799*BF4 + 0.0000222*BF5
−0.0003655*BF6 + 0.035452*BF7 − 0.0115093*BF8
−0.0000255*BF9 + 0.0001212*BF10 + 0.0005897*BF11
−0.0128733*BF12 − 0.0083235*MinHR
+0.0011797*BF15 − 0.0007934*BF16 + 0.0001375*BF17
−0.0012507*BF18 + 0.0010502*BF19 − 0.0002327*BF20
+0.0326878*BF21 − 0.0022148*BF22 + 0.1137366*BF23
+0.0099122*BF25 − 0.0014228*BF26 + 6.07E-06*BF27
−0.0002325*BF28 − 0.0000247*BF29 + 0.0009776*BF30
+4.516253 (*Model 1*)

Awake EE (kcal/min) = 0.0006482*BF1 − 0.0030562*BF2
+0.0299409*BF3 − 0.0492735*BF4 + 0.0000231*BF5
−0.0002731*BF6 + 0.0334973*BF7 − 0.0103561*BF8
−0.0000259*BF9 + 0.0000812*BF10 + 0.0004687*BF11
−0.0132276*BF12 + 0.0020462*BF13 − 0.0006229*BF14
−0.0053921*MinHR + 0.0004149*BF17
−0.0029474*BF18 + 0.0010143*BF19 − 0.0001699*BF20
+0.916625*BF21 − 0.0005704*BF23 − 0.0004599*BF24
+0.0093968*BF25 − 0.0018239*BF26 − 0.0001348*BF27
+0.0005261*BF28 + 0.0008766*BF29 + 0.0001015*BF30
+4.030813 (*Model 2*)

Sleep EE (kcal/min) = 0.0028321*BF1 − 0.014945*BF2
+0.0049603*BF3 + 0.0026882*BF5 − 0.0099002*BF6
−0.0702737*BF7 − 0.0096472*BF8 + 0.0035915*BF9
−0.0042611*BF10 − 0.0032241*MinHR
+0.0094646*BF13 − 0.0049867*BF16 − 0.0008203*BF17
−0.0001487*BF18 + 0.0000899*BF19 + 0.0001407*BF20
+0.0004735*BF21 − 0.0002574*BF22 + 0.0029634*BF23
+0.0001622*BF25 − 0.0000257*BF26
−0.0013074*BF29 + 0.0000528*BF30 + 1.744383
(*Model 3*)

Activity EE (kcal/min) = 0.0008375*BF1 − 0.0019102*BF2
+0.0000637*BF3 − 0.0000233*BF4 + 0.0183853*BF5
−0.0051662*BF6 + 0.0256539*BF7 − 0.0177271*BF8
+8.58e-06*BF9 − 0.0000967*BF10 + 0.0000128*BF11
−0.0001015*BF12 + 0.0000946*BF13 − 0.0002568*BF14
+0.0003504*BF15 − 0.0000104*BF16 − 7.02e
−06 * BF17 + 0.0000195*BF18 + 0.0004015*BF19
−0.0000711*BF20 − 0.0058478*MinHR
+0.0084682*BF25 − 2.94e − 06*BF27
−0.0000196*BF28
−0.0001167*BF29 − 0.0006037*BF30 + 1.314087
(*Model 4*)

MARS modeling program ranks independent variables in order of importance, based on the reduction in the goodness of fit. For the 24-h EE model, weight, HR *lead 2*, AC *lag 1*, AC, AC *lag 2*, height, HR *lag 2*, MinHR, sex, HR *lead 1*, and SitHR were ranked in descending importance. For awake EE, weight, HR *lead 2*, AC *lag 1*, AC *lag 2*, AC, height, sex, HR *lag 2*, MinHR, and SitHR were ranked in descending order. For sleep EE, weight, sex, AC *lag 2*, MinHR, height, age, AC *lag 1*, HR, HR *lead 2*, and HR *lead 1* were ranked in descending order. For activity EE, height, weight, HR *lead 2*, AC, AC *lag 1*, AC *lag 2*, MinHR, and sex were the important variables in descending order.

Evaluation of the MARS prediction models with the development cohort. Prediction errors of the 24-h EE, awake EE, sleep EE, and activity EE MARS models are presented for the development cohort in Table 4. The mean percent errors were 0.4 ± 7.3, 0.4 ± 7.2, 0.5 ± 6.4, and 1.5 ± 16.5% for the 24-h, awake, sleep, and activity EE models, respectively. In terms of root mean square error (RMSE), the values were 154, 122, 27, and 108 kcal for 24-h, awake, sleep, and activity periods, respectively. The CCC were 0.959, 0.960, 0.871, and 0.951 for the 24-h, awake, sleep, and activity EE models, respectively.

Application of the awake EE model made a minor reduction in the prediction errors. However, application of the sleep model halved the prediction errors in sleep EE. In addition, prediction errors also were evaluated when the awake EE and sleep EE MARS models were used to predict EE for the respective awake and sleep periods and are presented as the combined model in Table 4. The combined model performed similarly to the 24-h model.

Validation of the MARS prediction equation with an independent cohort. Prediction errors of the 24-h EE, awake EE, sleep EE, and activity EE MARS models are presented for the validation cohort in Table 5. The mean percent errors were −2.5 ± 7.5, −2.6 ± 7.8, −0.3 ± 8.9, and −11.9 ± 17.9% for the 24-h, awake, sleep, and activity EE models, respectively. The RMSE values were 168, 138, 40, and 122 kcal for 24-h, awake, sleep, and activity periods, respectively. The combined model for 24-h EE performed comparably to the 24-h model. In the validation cohort, 69% of the predicted TEE values for the 24-h model were within 10% of the observed TEE.

Bland-Altman plots of the differences between 24-h TEE observed in the room respiration calorimeter and predicted by the MARS model are presented for the development and validation cohorts in Fig. 2*A*. The Bland-Altman plots indicate

Table 5. *Prediction errors of the 24-h, awake, sleep, activity and combined MARS models presented as mean absolute error, percent error, and root mean square error in the validation cohort*

	Mean Absolute Error, kcal	Percent Error, %	Root Mean Square Error, kcal
24-h Model			
24-h TEE	−67.8 ± 154.7	−2.5 ± 7.5	167.8
Awake EE	−96.3 ± 131.9	−4.6 ± 8.2	162.5
Sleep EE	28.5 ± 50.8	6.1 ± 11.4	57.9
Awake model			
Awake EE	−59.8 ± 125.2	−2.6 ± 7.8	137.8
Sleep model			
Sleep EE	−4.9 ± 39.9	−0.3 ± 8.9	39.9
Activity model			
Activity EE	−65.7 ± 104.1	−11.9 ± 17.9	122.4
Combined model (awake + sleep) 24-h TEE	−64.7 ± 152.6	−2.3 ± 7.4	164.6

Values are means ± SD.

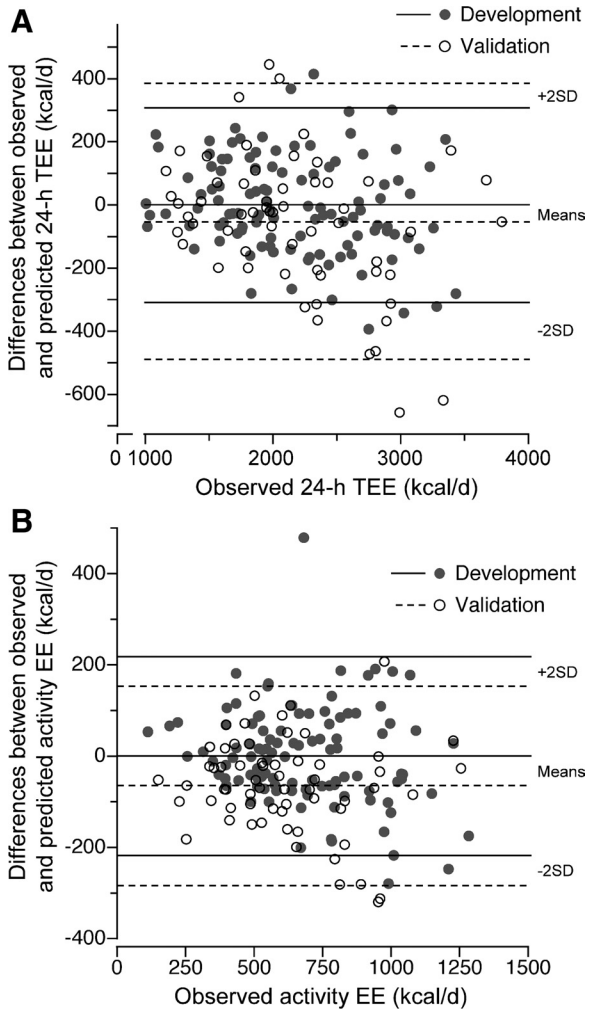

Fig. 2. Bland-Altman plots of the differences between EE (kcal/day) observed in the room respiration calorimeter and predicted by the 24-h (*A*) and activity EE (*B*) multivariate adaptive regression splines (MARS) models for the development and validation cohorts. TEE, total EE.

that the predicted values are in good agreement with the observed TEE. For the validation cohort, the mean absolute error was slightly negative, −67.8 kcal/day, due to a few outliers, compared with 0.0 kcal/day for the development cohort. The slopes for the Bland-Altman plot in Fig. 2*A* were −0.06 [$r^2 = 0.04$; nonsignificant (NS)] and −0.09 ($r^2 = 0.15$; $P < 0.05$) for the development and validation cohorts, respectively. While statistically significant for the validation cohort, we do not believe it is scientifically important, as indicated by r^2. Furthermore, the substantial overlap between the development and validation cohorts indicates concordant model performance in an independent data set. Likewise, the Bland-Altman plots for activity EE demonstrate that the predicted values are in good agreement without bias with the observed values in both cohorts (Fig. 2*B*). The slopes for the Bland-Altman plot in Fig. 2*B* were −0.081 ($r^2 = 0.03$; NS) and −0.061 ($r^2 = 0.02$; NS) for the development and validation cohorts, respectively.

Prediction errors for 24-h TEE were not statistically associated with age, sex, weight, height, or BMI. Differences in 24-h TEE observed in the room respiration calorimeter and predicted by the MARS model are displayed as a function of age for the development and validation cohorts in Fig. 3*A*. Differences between observed and predicted 24-h TEE as a function of sex and overweight status are presented for the development and validation cohorts in Fig. 3*B*.

Prediction errors using the 24-h model were computed for discrete physical activities (Table 6). The prediction errors expressed in EE (kcal/min) are displayed graphically in Fig. 4.

DISCUSSION

Accurate and precise population-specific models for the prediction of minute-by-minute EE, and hence TEE, awake EE, sleep EE, and activity EE from HR and AC, were constructed using MARS in children and adolescents. Based on known subject-specific predictors and physiological correlates of EE, MARS captured the complex metabolic and physiological processes that result in the production of EE. MARS is a multivariate nonparametric regression splines method that es-

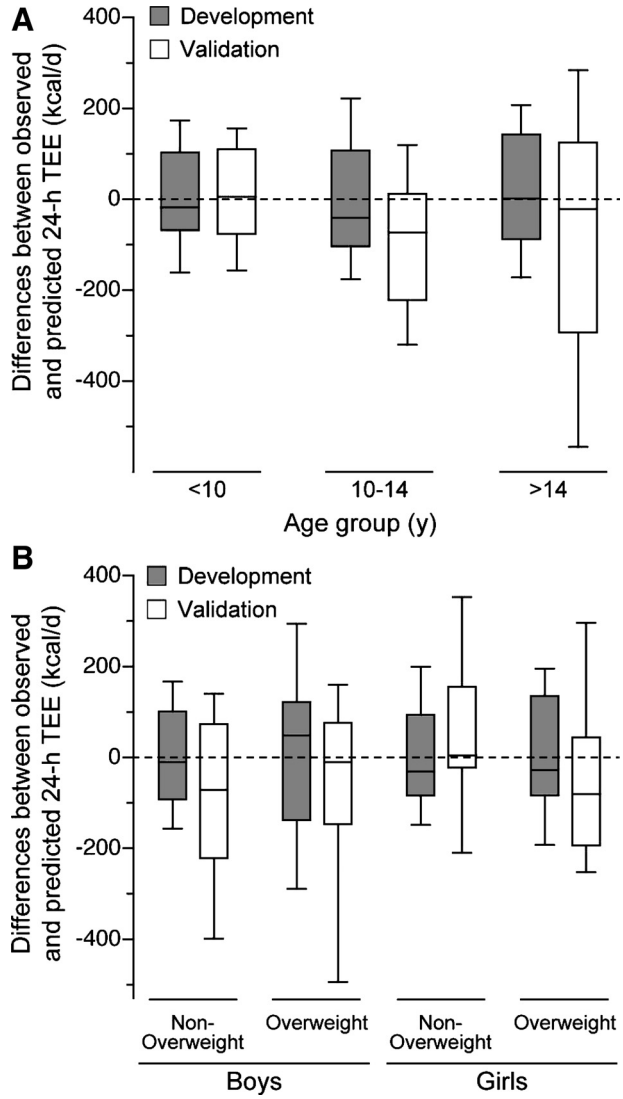

Fig. 3. Differences between 24-h TEE (kcal/day) observed in the room respiration calorimeter and predicted by the 24-h EE MARS model displayed as a function of age (*A*) and sex and overweight status (*B*) for the development and validation cohorts.

Table 6. *Prediction errors for discrete physical activities predicted by the 24-h MARS model in the development and validation cohorts*

	Development Cohort				Validation Cohort			
	Observed EE, kcal/min	Mean absolute error, kcal/min	Percent error, %	Root mean square error, kcal/min	Observed EE, kcal/min	Mean absolute error, kcal/min	Percent error, %	Root mean square error, kcal/min
Watching a movie	1.39 ± 0.36	0.01 ± 0.16	0.7 ± 11.3	0.16	1.46 ± 0.40	−0.04 ± 0.14	−2.1 ± 9.6	0.15
Computer/video games	1.29 ± 0.32	−0.03 ± 0.14	−2.0 ± 10.0	0.14	1.39 ± 0.37	−0.04 ± 0.16	−2.3 ± 12.4	0.16
EyeToy/Wii	2.92 ± 1.19	0.07 ± 0.42	4.9 ± 14.1	0.43	2.66 ± 0.99	−0.02 ± 0.34	1.3 ± 13.4	0.34
Aerobics/dance/DDR	4.14 ± 1.62	0.20 ± 0.54	6.7 ± 13.5	0.57	3.41 ± 1.34	−0.20 ± 0.43	−4.1 ± 11.5	0.47
Slow walk (1.8–3.0 mph)	3.11 ± 0.96	0.10 ± 0.36	3.7 ± 12.3	0.37	3.55 ± 1.45	0.01 ± 0.43	2.6 ± 11.4	0.42
Walk 2.5 mph	3.77 ± 1.27	−0.11 ± 0.43	−1.4 ± 11.3	0.44	3.99 ± 1.28	0.02 ± 0.43	2.4 ± 11.3	0.42
Fast walk/jog (3.5–8 mph)	6.70 ± 2.42	−0.24 ± 0.68	−2.6 ± 9.1	0.71	5.97 ± 3.37	−0.43 ± 1.01	−2.9 ± 12.2	1.09

Values are means ± SD. DDR, Dance Dance Revolution.

timates complex nonlinear relationships by a series of spline functions of the independent predictors and proved to be applicable to the field of EE. These MARS models represent a significant advancement in field methodology, since their application is laboratory calibration free and prediction errors are acceptable at the level of the individual and approach the errors for the doubly labeled water method in field applications estimated to be between 4 and 8% (17).

Our final MARS models for the prediction of EE from HR and AC were based on 23–28 basis functions, which utilized subject characteristics, HR and AC, 1- and 2-min lag and lead values of HR and AC, and appropriate interaction terms. Evaluation of the MARS models indicated high concordance or satisfactory fit to the data. The Bland-Altman plots demonstrated good agreement between the observed and predicted TEE and no systematic bias in TEE.

We partitioned TEE into awake and sleep periods to compare the performance of the 24-h EE and awake- and sleep-specific MARS models. Awake EE is the most variable component of TEE among individuals and the most challenging to predict, mostly because of many local features, such as peaks in the data and irregularities of HR and AC profiles. Time-varying variables of HR and AC allow us to distinguish individuals of the same age, sex, and body size, but different physical activity levels. In developing the MARS models, we found that the awake EE dominated the 24-h model in key features and thus the awake EE model performed similarly to the 24-h model. For the sleep period, we demonstrated that sleep EE can be predicted directly using our 24-h or sleep EE MARS models. If EE during sleep is of primary interest, the sleep-specific MARS model is more accurate and might be used. Oftentimes, BMR is predicted from weight and height using age- and sex-specific equations (18) and applied to the sleep period to predict sleep EE. This practice would introduce imprecision and systematic overestimation of sleep EE. For instance, in this study, BMR was 5 ± 7% higher than sleep EE. The combined model is probably not warranted, since the prediction of TEE was not substantially improved by the more complicated process of identifying the sleep and awake periods and applying the separate models for each period to obtain TEE.

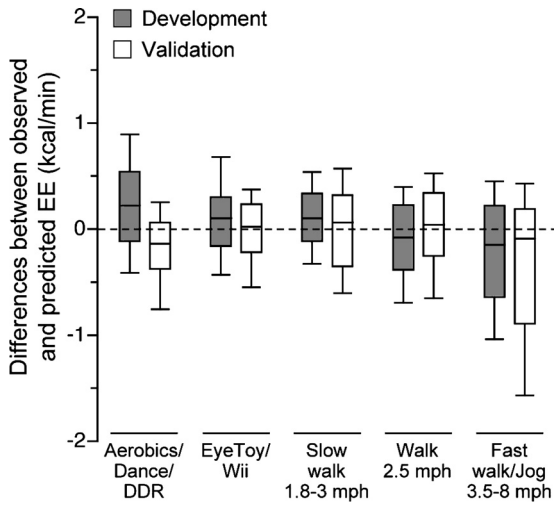

Fig. 4. Differences between EE (kcal/min) observed in the room respiration calorimeter and predicted by the 24-h EE MARS model for physical activities performed by the development and validation cohorts. DDR, Dance Dance Revolution.

In the field of physical activity monitoring, activity EE is of interest. Therefore, we also developed a model for the prediction of activity EE based on subject characteristics, HR and AC. Not surprisingly, activity EE closely tracks EE, since it is an affine transformation of EE. Although the RMSE (122 kcal) was similar to the RMSE for 24-h TEE and awake EE, the percent error was 17.9% due to the smaller denominator in the calculation for activity EE. Although our primary aim was to predict TEE from minute-by-minute EE, we examined errors in predicting EE during discrete physical activities to identify sources of error. Predicted EE of physical activities, on average, agreed within ±5% of observed values without any significant bias.

In our previous publication (25), we used CSTS analysis modeling for predicting minute-by-minute EE and hence TEE from HR and AC and other covariates using the present data set. CSTS is a parametric approach to model a collection of correlated data, taking into account within-individual changes and between-individual heterogeneity. CSTS takes advantage of this correlated structure in forecasting changes in EE based on previous and anticipated data. As in our MARS models, CSTS model incorporated the 1-min and 2-min lagged and lead values of HR or AC. For our population-specific CSTS model, the prediction errors and RMSE (kcal) for the development cohort were 0.9 ± 10.3% and 200.8 for TEE; 0.6 ± 9.9% and 162.4 for awake EE; 1.5 ± 8.7% and 36.6 for sleep EE; and 1.1 ± 16.0% and 107.7 for activity EE. For the CSTS model, the prediction

errors and RMSE for the validation cohort were −1.3 ± 9.9% and 223.7 for TEE; −1.9 ± 9.9% and 181.3 for awake EE; −0.5 ± 8.1% and 33.8 for sleep EE; and −8.2 ± 22.3% and 147.5 for activity EE. In general, the MARS predicted EE slightly better than the CSTS models, except for activity EE, in which case the errors were comparable.

Others also have applied advanced mathematical models to improve upon the prediction of EE using accelerometry and HR monitoring. Branched equation modeling was used to predict activity EE from HR and AC in adults (2) and children (4). In 12 men using Computer Science and Applications and Polar HR data, mean errors for activity EE during 24-h room calorimetry were −4.4 ± 29 and 3.5 ± 20.1% for individual and group calibration, respectively (2). In 145 children using Actiheart, the mean bias (RMSE) for six activities was −43.4 or −14.2% (115.6 $J \cdot kg^{-1} \cdot min^{-1}$) (4). In the latter study, systematic errors were present for discrete activities, with an overestimation during sedentary activities and an underestimation during jogging.

The novel application of MARS for processing HR and AC data demonstrates that minute-by-minute EE and hence TEE from HR and AC can be predicted accurately and precisely, with errors acceptable at the level of the individual child. Furthermore, our population-specific MARS models do not require individual laboratory calibration, enabling wide application in populations of children and adolescents. MARS models are now computationally feasible techniques, due to recent advances in statistical computing, and provide effective tools to obtain better predictive models for EE. Although the development of MARS models is mathematically complex, once developed, MARS models can be implemented easily in standard statistical programs. MARS modeling makes a significant contribution to field methodology for the estimation of EE.

In conclusion, we have developed and validated MARS models based on HR and AC against room respiration calorimetry for the prediction of 24-h EE, awake EE, sleep EE, and activity EE in children and adolescents. MARS modeling has provided an accurate predictive model of EE based on HR monitoring and accelerometry that requires further validation in independent, free-living populations.

REFERENCES

1. **Bland JM, Altman DG.** Statistical methods for assessing agreement between two methods of clinical measurement. *Lancet* 1: 307–310, 1986.
2. **Brage S, Brage N, Franks PW, Ekelund U, Wong MY, Andersen LB, Froberg K, Wareham NJ.** Branched equation modeling of simultaneous accelerometry and heart rate monitoring improves estimate of directly measured physical activity energy expenditure. *J Appl Physiol* 96: 343–351, 2004.
3. **Chen KY, Bassett DR Jr.** The technology of accelerometry-based activity monitors: current and future. *Med Sci Sports Exerc* 37: S490–S500, 2005.
4. **Corder K, Brage S, Ekelund U.** Accelerometers and pedometers: methodology and clinical application. *Curr Opin Clin Nutr Metab Care* 10: 597–603, 2007.
5. **Corder K, Brage S, Ekelund U.** Accelerometers and pedometers: methodology and clinical application. *Curr Opin Clin Nutr Metab Care* 10: 597–603, 2007.
6. **Craven P, Wahba G.** Smoothing noisy data with spline functions. Estimating the correct degree of smoothing by the method of generalized cross-validation. *Numerische Mathematik* 31: 317–403, 1979.
7. **Eubank RL.** *Nonparametric and Spline Smoothing***.** New York: Dekker, 1999.
8. **Friedman JH.** Multivariate adaptive regression plines (with discussion). In: *The Annals of Statistics*, 1991, p. 1–141.
9. **Hastie T, Tibshirani R, Friedman J.** *The Elements of Statistical Learning***.** New York: Springer-Verlag, 2001.
10. **Krippendorff K.** *Bivariate Agreement Coefficients for Reliability of Data***.** San Francisco, CA: Jossey Bass, 1970.
11. **Kuczmarski RJ, Ogden CL, Grummer-Strawn LM, Flegal KM, Guo SS, Wei R, Mei Z, Curtin LR, Roche AF, Johnson CL.** *CDC Growth Charts: United States. Advance Data From Vital and Health Statistics***.** Hyattsville, MD: US Department of Health and Human Services, 2000.
12. **Lin L.** A concordance correlation coefficient to evaluate reproducibility. *Biometrics* 45: 255–268, 1989.
13. **Lin L.** A note on the concordance correlation coefficient. *Biometrics* 56: 324–325, 2000.
14. **Moon JK, Butte NF.** Combined heart rate and activity improve estimates of oxygen consumption and carbon dioxide production rates. *J Appl Physiol* 81: 1754–1761, 1996.
15. **Moon JK, Vohra FA, Valerio Jimenez OS, Puyau MR, Butte NF.** Closed-loop control of carbon dioxide concentration and pressure improves response of room respiration calorimeters. *J Nutr* 125: 220–228, 1995.
16. **Rothney MP, Neumann M, Beziat A, Chen KY.** An artificial neural network model of energy expenditure using nonintegrated acceleration signals. *J Appl Physiol* 103: 1419–1427, 2007.
17. **Schoeller DA.** Energy expenditure from doubly labeled water: some fundamental considerations in humans. *Am J Clin Nutr* 38: 999–1005, 1983.
18. **Schofield WN, Schofield C, James WPT.** Basal metabolic rate–review and prediction, together with an annotated bibliography of source material. *Human Nutrition Clinical Nutrition* 39C: 1–96, 1985.
19. **Strath SJ, Bassett DR Jr, Thompson DL, Swartz AM.** Validity of the simultaneous heart rate-motion sensor technique for measuring energy expenditure. *Med Sci Sports Exerc* 34: 888–894, 2002.
20. **Strath SJ, Brage S, Ekelund U.** Integration of physiological and accelerometer data to improve physical activity assessment. *Med Sci Sports Exerc* 37: S563–S571, 2005.
21. **Treuth MS, Adolph AL, Butte NF.** Energy expenditure in children predicted from heart rate and activity calibrated against respiration calorimetry. *Am J Physiol Endocrinol Metab* 275: E12–E18, 1998.
22. **Venables WN, Ripley BD.** *Modern Applied Statistics with S.* New York: Springer-Verlag, 2002.
23. **Weir JB.** New methods for calculating metabolic rate with special reference to protein metabolism. *J Physiol* 109: 1–9, 1949.
24. **Westerterp KR.** Assessment of physical activity: a critical appraisal. *Eur J Appl Physiol* 105: 823–828, 2009.
25. **Zakeri I, Adolph AL, Puyau MR, Vohra FA, Butte NF.** Application of cross-sectional time series modeling for the prediction of energy expenditure from heart rate and accelerometry. *J Appl Physiol* 104: 1665–1673, 2008.
26. **Zhang K, Pi-Sunyer FX, Boozer CN.** Improving energy expenditure estimation for physical activity. *Med Sci Sports Exerc* 36: 883–889, 2004.
27. **Zhang K, Werner P, Sun M, Pi-Sunyer FX, Boozer CN.** Measurement of human daily physical activity. *Obes Res* 11: 33–40, 2003.